Predictability of the Power Output of Three Wave Energy Technologies in the Danish North Sea

Chozas, Julia Fernandez; Jensen, N. E. Helstrup; Sørensen, H. C.; Kofoed, Jens Peter; Kabuth, Alina Kristin

Published in:
9th ewtec 2011

Publication date:
2011

Document Version
Accepted author manuscript, peer reviewed version

Predictability of the Power Output of Three Wave Energy Technologies in the Danish North Sea

J. Fernández Chozas[1,2], N.E. Helstrup Jensen[3], H.C. Sørensen[1], J.P. Kofoed[2] and A. Kabuth[4]

[1] *Spok ApS*
Blegdamsvej 4, 2200 Copenhagen (Denmark)
julia@spok.dk; consult@spok.dk

[2] *Aalborg University, Department of Civil Engineering*
Sohngaardholmsvej 57, 9000 Aalborg (Denmark)
jfch@civil.aau.dk; jpk@civil.aau.dk

[3]*Energinet.dk*
Fredericia (Denmark)
neh@energinet.dk

[4]*University of Copenhagen, Department of Geography and Geology*
Copenhagen (Denmark)
akk@geo.ku.dk

Abstract— **The paper addresses an important challenge ahead the integration of the electricity generated by wave energy conversion technologies into the electric grid. Particularly, it looks into the role of wave energy within day-ahead electricity markets. For that the predictability of the theoretical power outputs of three wave energy technologies in the Danish North Sea are examined. The simultaneous and co-located forecast and buoy-measured wave parameters at Hanstholm, Denmark, during a non-consecutive autumn and winter 3-month period form the basis of the investigation.**

The objective of the study is to provide an indication on the accuracy of the forecast of i) wave parameters, ii) the normalised theoretical power productions from each of the selected technologies (Pelamis, Wave Dragon and Wavestar), and iii) the normalised theoretical power production of a combination of the three devices, during a very energetic time period.

Results show that for the 12 to 36 hours forecast horizon, the accuracy in the predictions (in terms of scatter index) of the significant wave height, zero crossing period and wave power are 22%, 11% and 74%, respectively; and the accuracy in the predictions of the normalised theoretical power outputs of Pelamis, Wave Dragon and Wavestar are 37%, 39% and 54%, respectively. The best compromise between forecast accuracy and mean power production results when considering the combined production of the three devices.

Keywords— Pelamis, Wave Dragon, Wavestar, Denmark, North Sea, Hanstholm, electricity markets, grid integration, power output, predictability, wave energy.

I. INTRODUCTION

As wave conversion technologies approach the commercial stage, it is necessary to investigate some of the issues ahead the integration of wave power into the electric grid. Above all, the paper focuses on the role of wave energy predictability within current electricity markets and their established rules [1].

Transmission System Operators (TSOs) have a major role in the functioning of electricity markets. They are the national bodies responsible for operating the grid and assuring the electricity demand is fulfilled. TSOs also publish the day-ahead load forecast and plan grid operation before real-time, generally one-day in advance.

In the case of Denmark, the day-ahead electricity market closes at 12 am. Thus, Energinet.dk as the Danish TSO requires the prediction of the following 12 to 36 hours electricity generation.

Electricity markets were first designed to accommodate conventional power generation. Besides hydropower, the contribution from renewable energy sources was scarce. Nowadays, as the percentage of renewable generation within the electricity mix increases [2], the uncertainty on the planned generation has also risen. The reason is that some of the most promising renewable energy sources such as wave power or wind power are not entirely predictable. This partial unpredictability is causing TSOs, producers and/or electricity users large expenditures to cope with the costs of the electric system balancing mechanisms [3].

Consequently, the paper examines waves predictability. It investigates the correlation of forecast and buoy-measured wave data as well as the correlation of forecast based and buoy-measured based theoretical power productions of three wave energy converters (WECs).

Corrected version of June 2012 of the paper with the same title presented at the European Wave and Tidal Energy Conference, EWTEC, 2011

The objective of this study is to provide some initial indication on the extent the power productions from WECs can be predicted 12 to 36 hours ahead for day-ahead markets. Moreover, waves forecasts play also a major role in the operation of WECs. It allows estimating and evaluating future power productions of a WEC, planning periods of tests and maintenance activities, and defining the storm protection strategy, if needed.

The study is based on available simultaneous and co-located forecast and buoy-measured wave data from Hanstholm site, Denmark, during a 5-month period. Also the power matrices of the selected devices form the basis of the study. The WECs chosen are Pelamis [4], an offshore floating heaving and pitching articulated converter, Wave Dragon [5], an offshore floating overtopping technology and Wavestar [6], a near-shore multi-point absorber.

This paper presents the first approach of the Danish TSO towards the study of predictability of WECs' power output. The novelties of this paper are first, examining wave parameters predictability; second, comparing forecast based and buoy-measured based theoretical power productions; third, considering the separated as well as the combined power outputs of three different WECs, and fourth, locating the study in the North Sea waters, an area with increasing interest on wave energy [7].

The content of the paper is as follows:

i) Methodology of the study;
ii) Results of the study in terms of forecast accuracy of wave parameters and of forecast accuracy of theoretical power productions of the devices;
iii) Discussion of results and limitations of the study;
iv) Conclusions and further recommended work.

II. Methodology

A. Time period

The analysis embraces three complete and non-consecutive months of wave measurements. The overall period covers from end of October 2010 to middle of February 2011; valid data is from 26/10 to 20/11/2010, from 11/12/2010 to 13/01/2011 and from 16/01 to 09/02/2011. All times and dates are expressed in the Coordinated Universal Time (UTC) system.

Generally at Hanstholm, January is the month with the most energetic wave climate, about 6 times more in terms of monthly mean wave power than the less energetic months, April, May, June and July [8]. Therefore, the time period considered in this study represents the most energetic season.

B. Wave parameters

Different environmental parameters such as wave height, wave period, wave direction, wind speed, wind direction, water depth or current speed fully characterize the environmental conditions at a particular location. However, as a first analysis, it is suitable to define the wave resource by the significant wave height H_s and the zero crossing period T_z. These parameters have been approximated by H_{m0} and T_{02}, respectively [9].

The power output of a device is also influenced by some of these environmental features, the degree of influence depending on the working principle. An accurate performance evaluation requires the inclusion of several parameters although a WEC is also well defined by H_{m0} and T_{02}.

As a result, this study is based on records of H_{m0} and T_{02}. The maximum wave height H_{max} has also been included, since its evaluation can lead to useful results on buoy measurement errors and WECs' operation and survivability conditions.

C. Study Location - Hanstholm

The selected research site is Hanstholm, at the west coast of Jutland, Denmark, in the Danish part of the North Sea. The long term mean energy flux is estimated at 7 kW/m at water depths of 17 meters coming primarily from West-North-West and West direction, and the 10 years design wave height is 6.6 meters [10-11]. The wave climate is characterized by a wind sea on top of a non-constant swell arriving from the northern part of the Atlantic Ocean.

The study refers to a point approx. 1.5 km offshore and at 17 m water depths (coordinates 8.5821°E, 57.1315°N).

Fig. 1 depicts the wave conditions at this site throughout the study period, in terms of H_{m0}, T_{02} and the contribution of each sea state, in percentage, to the mean wave power in the study period. The scatter diagram is based on buoy-measurements of H_{m0} and T_{02} over 4 months. It shows a dominant wind sea with a peak at H_{m0}= 2.2 m and T_{02}= 5.3 s and a secondary peak at H_{m0}= 4 m and T_{02}= 6.5 s.

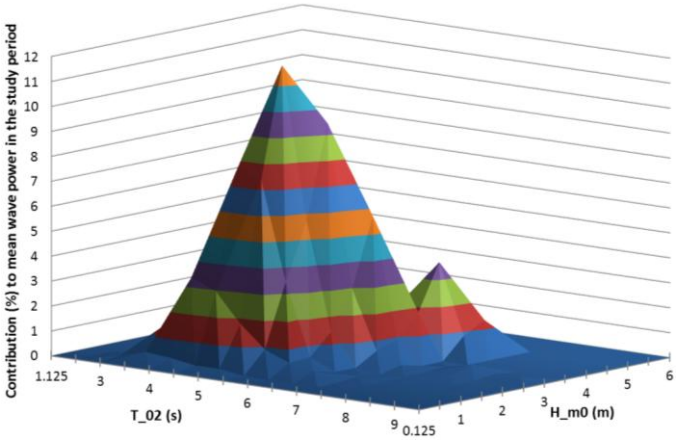

Fig. 1. Scatter Diagram of Hanstholm throughout the study period in terms of H_{m0}, T_{02} and contribution in percentage of each sea state to the mean wave power in the study period.

The wave conditions of the study period provide a valid representation of the long-term wave climate at Hanstholm. However, the mean wave power in this period, 8.9 kW/m, is higher than the mean annual wave power, 7 kW/m, due to the strong seasonal variability of the wave conditions at Hanstholm. Table I presents the probability of occurrence of the different wave parameters H_{m0}, H_{max}, T_{02} and wave power P_{wave} at Hanstholm in this period.

P_{wave} (power per unit of crest width) has been calculated according to the wave power density formula:

$$P_{wave}(W/m) = \frac{1}{16}\rho g H_{m0}^{2} \cdot C_g$$

where C_g is the group velocity, defined by:

$$C_g(m/s) = \frac{1}{2}\left[1 + \frac{2kd}{\sinh(2kd)}\right] \cdot \frac{gT_e}{2\pi} \cdot \tanh(kd)$$

k (m^{-1}) = $2\pi/L$ is the wave number
L (m) = $g*T_e^2/(2\pi)* \tanh(kd)$ is the wave length

For Hanstholm the following values have been considered:

- $\rho_{salt\ water}$ = *1027* kg/m^3 represents the water density considering an average water salinity concentration of 33 ppm and an average water temperature of 7 °C.
- g = *9.82* m/s^2 represents the gravity acceleration
- d = *17.5 m* represents the water depth
- $T_e = 1.2T_{02}$, represents the energy period. The equality is true assuming a Pierson-Moskowitz spectral shape [10].

Hanstholm location has been selected due to several positive reasons, although it also brings some limitations.

On one hand, there are comprehensive data sets of simultaneous and co-located half-hourly forecast and buoy-measured wave data. Moreover, there is an increasing interest on the characteristics at this particular location. A new wave energy test site named DanWEC, the Danish Wave Energy Centre [12] has been established, where a 1:2 scale model of Wavestar and a 1:5 scale model of Dexa Wave [13] are currently deployed. These prototype tests can complement the present study by providing actual power production data.

On the other hand, the wave potential at Hanstholm is limited compared to other interesting deployment sites. In addition, the three WECs selected have not been optimized for the wave climate of the North Sea, characterised by shorter period waves than the Atlantic Ocean longer period swells.

D. Forecast and Buoy-Measured Data

Wave forecasts have been calculated by the spectral wave module of MIKE 21 from the Danish Hydraulic Institute, a model based on the wave action conservation equation. The service is part of The Water Forecast program [14]. The forecast reaches 5 days into the future, is calculated every 12 hours and provides half-hour records of the main wave parameters with 2 decimals resolution.

Environmental measurements have been provided by a Datawell Waverider buoy from The Danish Coastal Authority (i.e. Kystdirektoratet). Data consists of half-hour records of H_{m0}, T_{02} and H_{max} with 2 decimals resolution.

The data sets of forecast H_{m0} and T_{02}, and buoy-measured H_{m0} and T_{02} have been used to develop time series of forecast P_{wave} and buoy-measured P_{wave}, respectively.

A variable has been introduced into the study to compare the forecasts to the measured data. *T-hour* represents the forecast hour or the time horizon, in hours, before real time. In other words, it is the time-span, in hours, between the forecast is calculated and the buoy measures the corresponding parameters.

E. Quality indices

Verification of forecast data against buoy-measured data can be quantified by the quality indices described below, where *MOD* corresponds to modeled, calculated or forecast data and *OBS* to observed or buoy-measured data.

The *Mean* value of observations is defined as:

$$Mean = \frac{1}{N}\sum_{i=1}^{N} OBS_i$$

where N corresponds to the number of valid observations.

The mean of difference or *Bias* represents an error that remains primarily constant in magnitude for all forecasts. It is defined as:

$$Bias = \frac{1}{N}\sum_{i=1}^{N} (MOD - OBS)_i$$

The mean of absolute difference or *MAE* is defined as:

$$MAE = \frac{1}{N}\sum_{i=1}^{N} (|MOD - OBS|)_i$$

The root mean square of difference or *RMSE* is calculated assuming a normal distribution and represents the standard deviation of the mean (confidence level of 68.27%). It is defined as:

$$RMSE = \sqrt{\frac{1}{N}\sum_{i=1}^{N} (MOD - OBS)_i^2}$$

The unbiased scatter index or $SI_{unbiased}$ is also calculated assuming a normal distribution. It provides a non-dimensional measure of the error and is defined as:

$$SI_{unbiased} = \frac{\sqrt{\frac{1}{N}\sum_{i=1}^{N} (MOD - OBS - Bias)_i^2}}{Mean}$$

The correlation coefficient or *CC* indicates the degree to which the variation in one parameter is reflected in the variation of the other parameter. It is a non-dimensional variable ranging from 0 to 1, the former indicating no correlation between the two data sets and the latter perfect correlation. It is defined as:

$$CC = \frac{\sum_{i=1}^{N} (MOD_i - \overline{MOD})(OBS_i - Mean)}{\sqrt{\sum_{i=1}^{N} (MOD_i - \overline{MOD})^2 \sum_{i=1}^{N} (OBS_i - Mean)^2}}$$

F. *Wave converters – Pelamis, Wave Dragon and Wavestar*

To take advantage of the variability of the wave resource along the coasts it is generally expected that several wave conversion solutions remain attractive for the market. Moreover, to extend the scope of this study towards different WECs responses to the wave climate as well as to consider the differences in the operating conditions among the existing WECs, three different technologies have been selected for the study. These are:

1) *Pelamis*, a floating heaving and pitching converter.
2) *Wave Dragon*, an offshore floating overtopping device.
3) *Wavestar*, a near-shore multi-point absorber.

Power productions (P_{prod}) of the three WECs have been modeled from forecast and buoy-measured wave data. This process has required the application of a transfer function, i.e. a power matrix that represents the performance of the WEC at Hanstholm.

In this way, the records of forecast H_{m0} and T_{02}, and buoy-measured H_{m0} and T_{02} along with the power matrixes have been used to model time series of forecast P_{prod} and buoy-measured P_{prod}, respectively.

Whereas Wavestar provided a power matrix particularly developed for Hanstholm wave climate, those for Pelamis and Wave Dragon have been down-scaled from [15] to match the predominant sea states (Table I) and to optimize their P_{prod} in the study period.

Table II presents the scale factor, main dimensions and the peak power of the three devices, as well as the design sea states i.e. H_{m0} and T_{02} where they reach full production, and the operating limits of each device (minimum and maximum H_{m0} and T_{02}). Table II shows Wavestar cuts-off production in lower sea states than Pelamis or Wave Dragon.

Fig. 2 presents a comparison between the probability of occurrence of different sea conditions (defined by the contribution in percentage of H_{m0} and T_{02} to the mean wave power) and power production's dependency on these conditions. Fig. 2 shows that Wavestar has the best correlation between maximum P_{prod} and probability of occurrence of the wave parameter T_{02}.

Throughout the study the power productions of the three WECs are given as percentages of peak power, i.e. as normalized or non-dimensional values.

TABLE I
OCCURRENCE OF WAVE PARAMETERS H_{M0}, H_{MAX}, T_{02} AND P_{WAVE} AT HANSTHOLM THROUGHOUT THE STUDY PERIOD

	Mean	Max	<1% time	<10% time	<10% time	<1% time	Days	N
H_{m0} (m)	1.4	4.7	≤ 0.4	≤ 0.7	≥ 2.3	≥ 3.7	87	4157
H_{max} (m)	2.4	8.5	≤ 0.7	≤ 1.1	≥ 3.8	≥ 6.0	87	4157
T_{02} (s)	4.7	8.8	≤ 3.1	≤ 3.8	≥ 5.7	≥ 6.7	87	4157
P_{wave} (kW/m)	8.9	98.6	≤ 0.4	≤ 1.3	≥ 19.6	≥ 58.4	87	4157

TABLE II
SCALING RATIO, DIMENSIONS, PEAK POWER AND DESIGN AND OPERATING SEA STATES FOR PELAMIS, WAVE DRAGON AND WAVESTAR AT HANSTHOLM

	Ratio* (λ)	Main dimensions* (m)		Peak power (kW)	Design H_{m0} (m)	Design T_{02} (s)	H_{m0} min (m)	H_{m0} max (m)	T_{02} min (s)	T_{02} max (s)
Pelamis	1: 1.76	*l*=102	Ø= 2.3	100	3.1	4.6	0.4	5	2.5	10
Wave Dragon	1:1.76	*l*= 96	*w*=170	1000	3	5	0.4	5	2.6	10
Wavestar	1:2	---	Ø = 5	600	2.5	3.4	0.5	3	2	13

* Pelamis and Wave Dragon scaling ratios are relative to the Atlantic Ocean and Wavestar's to the North Sea. *l* represents length, *w* width and Ø diameter.

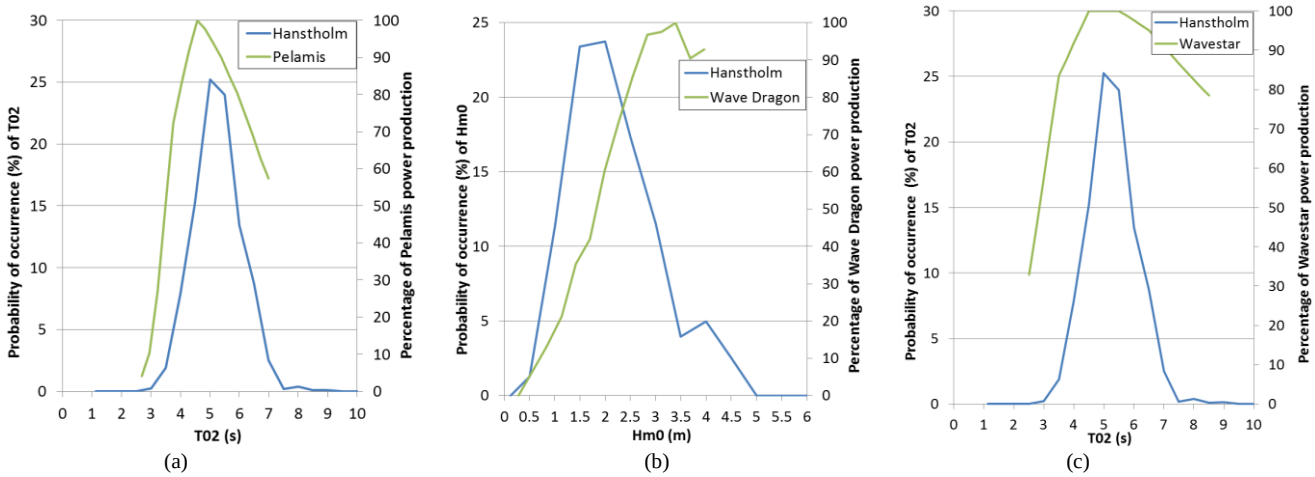

(a) (b) (c)

Fig. 2. Contribution, in percentage, of T_{02} and H_{m0} to the mean wave power at Hanstholm throughout the study period and normalised power productions of Pelamis (a), Wave Dragon (b) and Wavestar (c) in terms of T_{02} (a)-(c) and H_{m0} (b). Wave Dragon performance is more dependent on the variations of the wave height whereas Pelamis and Wavestar performances are more dependent on the period.

G. Further Assumptions

- The current delay in the forecast has been disregarded. At present, due to the research purpose of this study, the model delivers the forecast with 19-hour delay. In real implementation of forecast data this delay can be reduced.
- Errors in the buoy acquisition system have been disregarded.
- WECs' power production dependency on wave directionality has been neglected.
- Real power production data from the half scale Wavestar operating at Hanstholm have not been used in the study. All stated power productions are theoretical and derived from the power matrixes.

III. Results

To investigate forecast accuracy of WECs' theoretical power productions the predictability of the typical wave parameters is examined first.

Consequently, this section presents two sets of results. First, the error statistics obtained from the comparison of forecast H_{m0}, H_{max}, T_{02} and P_{wave} and buoy-measured H_{m0}, H_{max}, T_{02} and P_{wave}. Second, the error statistics obtained from the comparison of P_{prod} based on forecast data and P_{prod} based on buoy-measurements of each WEC and of a combination of them.

A. Predictability of Wave Parameters

Table III to Table VI show the quality indices, as defined in section II-D, for H_{m0}, H_{max}, T_{02} and P_{wave}, respectively. Forecast accuracy is evaluated for *T-hours* embracing 0 to 1 hour, 12 to 24 hours, 24 to 36 hours, 84 to 96 hours and 0 to 144 hours.

TABLE III
H_{M0} Quality Indices Throughout the Study Period

T - hour (h)		Mean (m)	Bias (m)	MAE (m)	RMSE (m)	$SI_{unbiased}$	CC	N
≥ 0	< 12	1.5	0.19	0.25	0.32	18%	0.94	4015
≥ 12	< 24	1.5	0.19	0.27	0.34	20%	0.91	3991
≥ 24	< 36	1.5	0.17	0.29	0.37	22%	0.89	3967
≥ 36	< 48	1.5	0.18	0.30	0.40	25%	0.86	3943
≥ 84	< 96	1.5	0.18	0.40	0.54	35%	0.72	3847
≥ 0	**< 144**	**1.5**	**0.20**	**0.36**	**0.48**	**30%**	**0.79**	41527

TABLE IV
H_{MAX} Quality Indices Throughout the Study Period

T - hour (h)		Mean (m)	Bias (m)	MAE (m)	RMSE (m)	$SI_{unbiased}$	CC	N
≥ 0	< 12	2.4	0.82	0.85	0.99	23%	0.92	4015
≥ 12	< 24	2.4	0.82	0.87	1.02	25%	0.90	3991
≥ 24	< 36	2.4	0.80	0.86	1.04	28%	0.87	3967
≥ 36	< 48	2.4	0.82	0.89	1.08	30%	0.85	3943
≥ 84	< 96	2.4	0.80	1.00	1.25	40%	0.69	3847
≥ 0	**< 144**	**2.4**	**0.85**	**0.97**	**1.20**	**36%**	**0.77**	41527

TABLE V
T_{02} Quality Indices Throughout the Study Period

T - hour (h)		Mean (s)	Bias (s)	MAE (s)	RMSE (s)	$SI_{unbiased}$	CC	N
≥ 0	< 12	4.7	-0.17	0.36	0.49	10%	0.81	4015
≥ 12	< 24	4.7	-0.16	0.38	0.51	10%	0.80	3991
≥ 24	< 36	4.7	-0.17	0.42	0.55	11%	0.77	3967
≥ 36	< 48	4.7	-0.17	0.43	0.56	11%	0.75	3943
≥ 84	< 96	4.7	-0.20	0.51	0.68	14%	0.62	3847
≥ 0	**< 144**	**4.7**	**-0.18**	**0.47**	**0.62**	**13%**	**0.68**	41527

TABLE VI
P_{WAVE} Quality Indices Throughout the Study Period

T - hour (h)		Mean (kW/m)	Bias (kW/m)	MAE (kW/m)	RMSE (kW/m)	$SI_{unbiased}$	CC
≥ 0	< 12	8.8	1.96	3.15	6.42	69%	0.91
≥ 12	< 24	8.8	1.94	3.33	6.28	68%	0.90
≥ 24	< 36	8.9	1.62	3.59	6.70	73%	0.86
≥ 36	< 48	8.9	1.58	3.88	7.26	80%	0.82
≥ 84	< 96	8.9	1.16	5.13	9.68	108%	0.64
≥ 0	**< 144**	**8.9**	**1.81**	**4.62**	**8.82**	**97%**	**0.75**

The following figures present a comparison between forecast H_{m0} and buoy-measured H_{m0} during the most energetic month (11/12/2010 to 11/01/2011). Fig. 3 illustrates the forecast for a *T-hour* of 12 hours, Fig. 4 for a *T-hour* of 36 hours and Fig. 5 for a *T-hour* of 108 hours. Note the big waves passing Hanstholm on 12/12/2010 and on New Year's Eve.

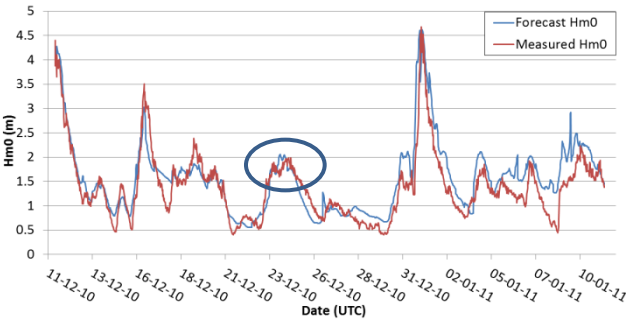

Fig. 3. H_{m0} comparison of measured (in red) and 12-hour forecast (in blue)

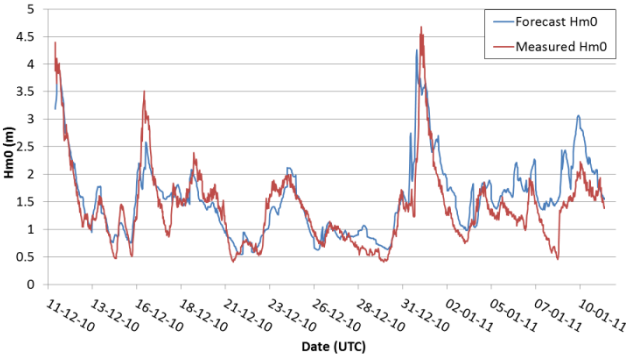

Fig. 4. H_{m0} comparison of measured (in red) and 36-hour forecast (in blue)

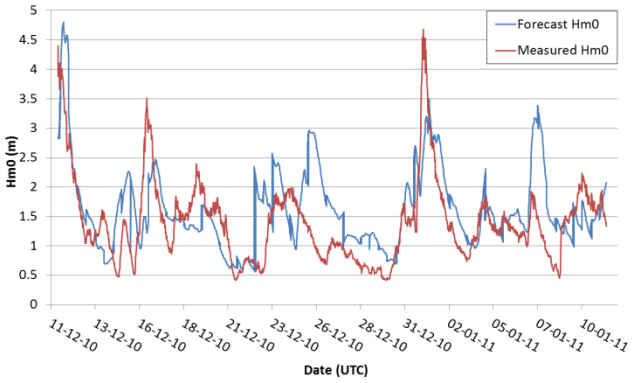

Fig. 5. H_{m0} comparison of measured (in red) and 108-hour forecast (in blue)

Fig. 6 presents a comparison between forecast T_{02} and buoy-measured T_{02} and Fig. 7 between forecast based P_{wave} and buoy-measured based P_{wave}, during the same month (11/12/2010 to 14/01/2011) for a *T-hour* of 12 hours.

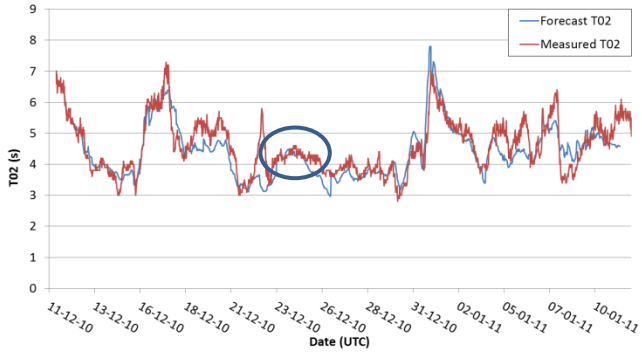

Fig. 6. T_{02} comparison of measured (in red) and 12-hour forecast (in blue)

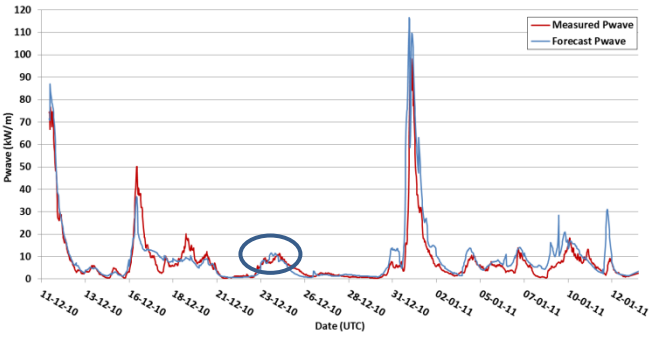

Fig. 7. P_{wave} comparison of measured (in red) and 12-hour forecast (in blue)

The circles in Fig. 3, Fig. 6 and Fig. 7 show the 3-day period selected in the next section to illustrate the evolution of the power productions for the three devices. These days provide a good representation of the typical operating conditions at the research site.

B. Predictability of WECs' Power Production

To evaluate power productions predictability normalized quality indices are used, which are normalized in terms of peak power (Table II). They are indicated by an "*N*" at the beginning of the parameter (i.e. *NBias*, *NMAE*, *NRMSE*).

Table VII presents the quality indices evaluating P_{prod} based on forecast data and P_{prod} based on buoy-measurements for each of the selected WECs and for the combination of the three of them. The 12 to 36 hours forecast has been considered. The 'combined' option reflects the contribution of one normalised unit of each technology.

TABLE VII
PELAMIS, WAVE DRAGON, WAVESTAR AND COMBINED NORMALISED P_{PROD} QUALITY INDICES THROUGHOUT THE STUDY PERIOD

	NMean	**NBias**	**NMAE**	**NRMSE**	**$SI_{unbiased}$**	N
Pelamis	0.33	0.08	0.11	0.14	0.37	11901
Wave Dragon	0.33	0.04	0.09	0.13	0.39	11901
Wavestar	0.44	0.04	0.15	0.24	0.54	11901
Combined	0.37	0.05	0.11	0.14	0.36	11901

Fig. 8 to Fig. 10 give a graphical representation of the differences between forecast P_{prod} and theoretical P_{prod} of Pelamis, Wave Dragon, Wavestar and the combination of the three devices. The graphs cover a 3-day period (23/12 to 25/12/2010). Fig. 8 depicts the 12 hours forecast and Fig. 9 the 36 hours forecast for the power production of Pelamis, Wave Dragon and Wavestar.

Fig. 10 illustrates the differences of the 12, 24 and 36 hours P_{prod} forecast to the theoretical P_{prod} for the combination of the three devices.

For comparison Fig. 11 shows the variation of the 12 hours forecast H_{m0}, T_{02} and P_{wave} and buoy-measured H_{m0}, T_{02} and P_{wave} over this 3-day period. Note that buoy-measured H_{m0}, T_{02} and P_{wave} vary around their mean values, as shown in Table I.

IV. DISCUSSION

Due to the scope of the paper only the results for a *T-hour* varying from 12 to 36 hours are discussed.

A. Location

The results presented in the study on predictability of wave parameters and power productions are dependent on the wave climate of the chosen location. A wave climate characterized by swells will significantly improve the accuracy in the predictions, since swells are more regular compared to wind seas. In a wind sea, where the correspondence between waves and wind patterns reveals to be high [16], the short-term forecast errors in wind are more reflected in wave predictions.

B. Predictability of Wave Parameters

1) Significant wave height spectral estimate H_{m0}: Table III shows the error statistics obtained from the comparison of forecast H_{m0} and buoy-measured H_{m0} for different *T-hours*.

The positive *Bias* indicates a prevalent trend where the forecast overestimates the buoy-measured values. Then, a *MAE* larger in magnitude than the *Bias* denotes that also the opposite trend is found, i.e. the forecast also underestimates the buoy-measured values, particularly as *T-hour* increases (Fig. 3 to Fig. 5).

RMSE points out that 68% of the forecasts are within ±0.35 meters of the *Mean* measured value of H_{m0}, i.e. 1.5 *meters*.

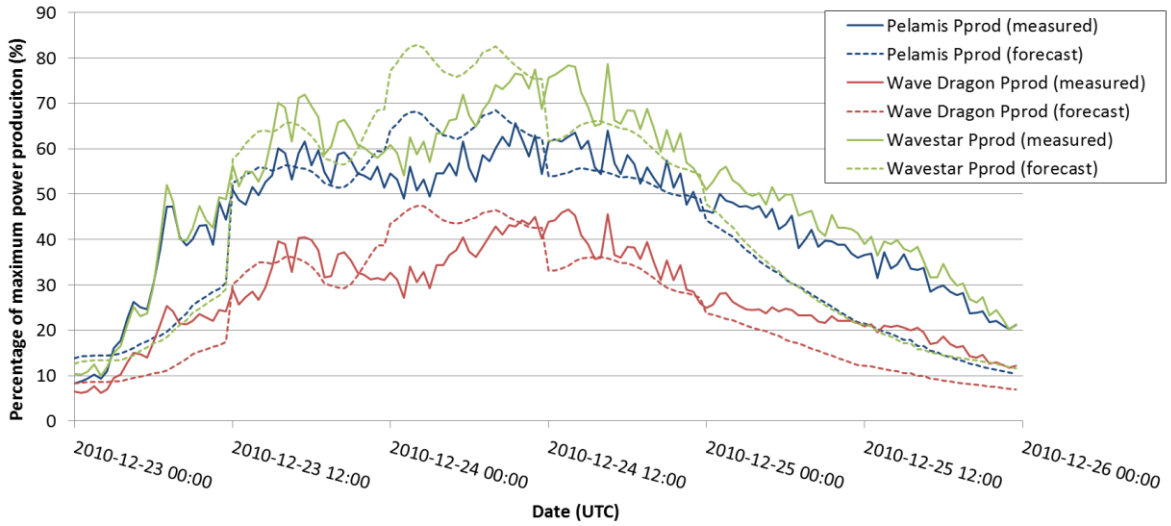

Fig. 8. P_{prod} based on buoy-measurements (solid lines) and P_{prod} based on forecast data (dashed lines), in terms of percentage of peak power of Pelamis (in blue), Wave Dragon (in red) and Wavestar (in green) for a *T-hour* of 12 hours over a 3-day period (23/12 to 25/12/2010).

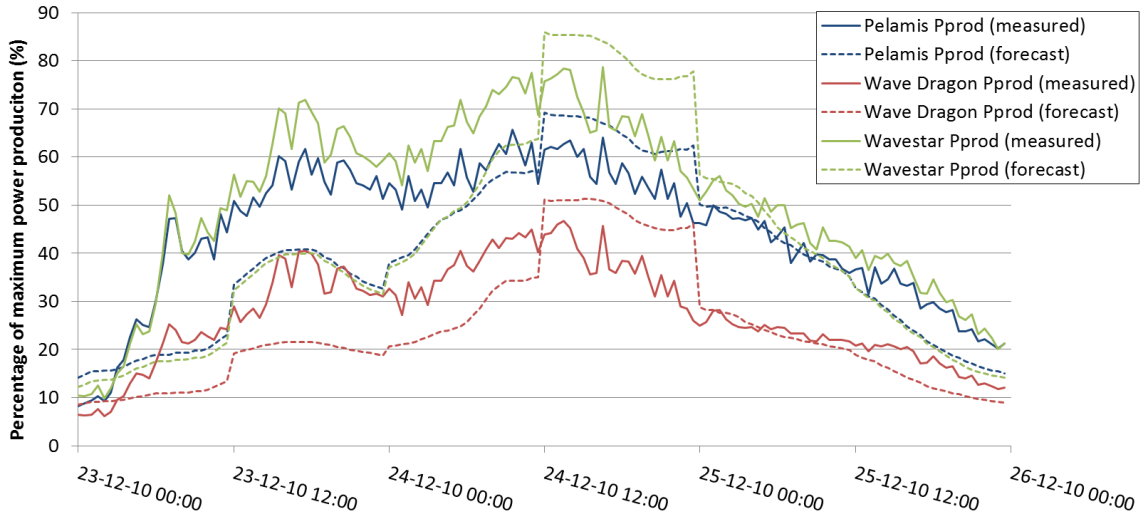

Fig. 9. P_{prod} based on buoy-measurements (solid lines) and P_{prod} based on forecast data (dashed lines), in terms of percentage of peak power of Pelamis (in blue), Wave Dragon (in red) and Wavestar (in green) for *T-hour* of 36 hours over a 3-day period (23/12 to 25/12/2010).

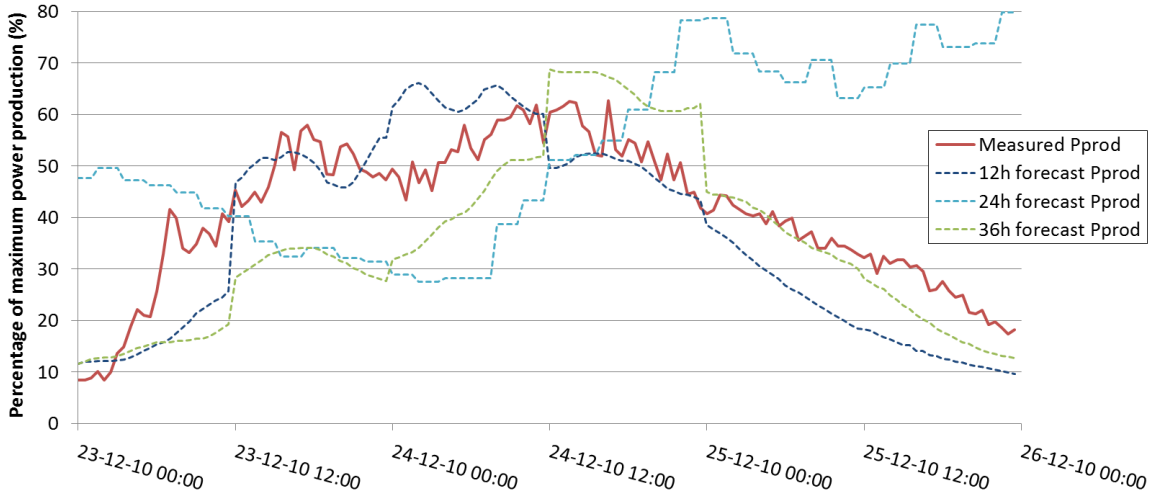

Fig 10. P_{prod} based on buoy-measurements (solid line) and P_{prod} based on forecast data (dashed lines), in terms of percentage of peak power of the combination of the three WECs, for a *T-hour* of 12 hours (dark blue), 24 hours (light blue) and 36 hours (green) over a 3-day period (23/12 to 25/12/2010).

A 22% $SI_{unbiased}$ illustrates an acceptable dispersion of the distribution. Then, a CC of 0.89 suggests a high correlation between the two sets of compared values.

In brief, results show that the agreement between H_{m0} forecasts and H_{m0} buoy-measured data is good.

2) Maximum wave height spectral estimate H_{max}: Table IV shows the error statistics obtained from the comparison of forecast H_{max} and buoy-measured H_{max} for different *T-hours.*

Errors for H_{max} forecasting are always higher than for H_{m0}, although the quality indices follow the same trend.. These errors may be provided by the buoy-measured data. A known disadvantage of the spherical buoys (e.g. Datawell Waverider buoy) is that due to the single line mooring, it circles around the crests of steep waves and thus, does not reach the maxima in the surface elevation [17].

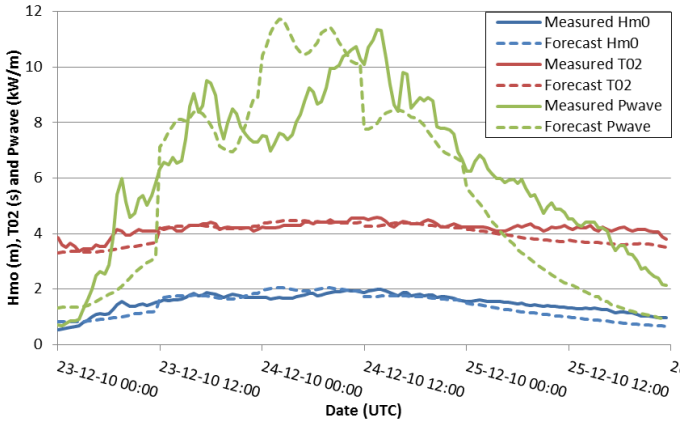

Fig. 11 Evolution of buoy-measured (solid line) and 12-hour forecast (dashed line) of H_{m0} (blue), T_{02} (red) and P_{wave} (green) over 23/12 to 25/12/2010.

3) *Zero crossing period spectral estimate T_{02}:* Table V shows the error statistics obtained from the comparison of forecast T_{02} and buoy-measured T_{02} for different *T-hours*.

The negative *Bias* indicates a prevalent trend where the forecast underestimates the buoy-measured value. A *MAE* more than twice the *Bias* denotes that the forecast also overestimates the measured values. However, both the *Bias* and *MAE* are small in magnitude compared to the *Mean*.

RMSE indicates that 68% of the forecasts are within ±0.55 seconds of the *Mean* measured value of T_{02}, i.e. 4.7 seconds.

The graphical comparison (Fig. 6) illustrates the small and very acceptable dispersion of the distribution, which lies within small bounds ($SI_{unbiased}$ of 11%).

The correlation between forecast and buoy-measured values (*CC*= 0.77) is lower than for H_{m0}. This can be clearly seen in Fig. 6, where the pattern tendencies of the buoy-measured values are not strictly followed by the forecasts.

In summary, results show that T_{02} forecast and T_{02} buoy-measurements are in very good agreement but for CC.

4) *Wave Power P_{wave}:* Table VI shows the error statistics obtained from the comparison of forecast P_{wave} and buoy-measured P_{wave} for different *T-hours*.

In this case, it is important to note the relation of P_{wave} with H_{m0} and T_{02}. The errors in H_{m0} get raised to the power of two and in T_{02} to the power of one.

The positive *Bias* reveals the strongest influence of H_{m0}. It indicates that the forecast overestimates the derived buoy-measured value. As happens also in the case of H_{m0} and T_{02}, *MAE* is larger than the *Bias*, so the forecast also underestimates the buoy-measured values. Both *Bias* and *MAE* are quite large in magnitude compared to the *Mean*.

RMSE indicates that 68% of the forecasts are within ±6.8 kW/m of the *Mean* measured value of P_{wave}, i.e. 8.9 kW/m. This value suggests an inaccurate forecast; however, it is due to the peaks in $P_{wave,}$ which can reach up to 99 kW/m at certain periods (Table I and Fig. 7). Similarly, the $SI_{unbiased}$ shows a 75% dispersion of the distribution.

On the contrary, the correlation (*CC*= 0.86) between forecast and buoy-measured values is high, induced by the high *CC* of H_{m0}.

Fig. 7 illustrates the peaks in P_{wave} in comparison to the *Mean* average value of 8.9 kW/m. This difference explains the high value of *RMSE* and $SI_{unbiased}$.

In short, results show that P_{wave} forecast derived and P_{wave} buoy-measured derived are in good agreement for small P_{wave} values but not for larger ones.

As a summary, wave parameters predictability can be considered accurate for H_{m0} and T_{02}, acceptable for H_{max} and for values of P_{wave} close to the mean, and not very accurate for larger P_{wave} values.

C. Predictability of WECs' Power Production

1) *Pelamis, Wave Dragon and Wavestar:* Table VII shows the error statistics obtained from the comparison of normalised P_{prod} based on forecast data and normalised P_{prod} based on buoy-measurements for the three devices.

The figures illustrate similar trends in the quality indices of each device. However, for comparison note the normalised mean production of Wavestar is approx. 7% larger than that of Pelamis and Wave Dragon.

Forecast accuracy of Pelamis and Wave Dragon production are comparable. The main difference is that whereas the $SI_{unbiased}$ of Pelamis (37%) is better than for Wave Dragon (39%), the *NMAE* favours Wave Dragon (9% versus 11% for Pelamis).

Then, Wavestar presents larger standard deviation (*NRMSE*= 24%) and dispersion ($SI_{unbiased}$= 54%), although the normalised mean production reaches 44% of peak power. Hence, *NMAE* (15%) is comparable to the others.

In the three cases, the positive *NBias* suggests an influence of H_{m0} forecast errors on the power production calculations. The *NMAE* also indicates the influence from T_{02} forecast errors, particularly for Wavestar.

For the three devices, *NRMSE* reveals to be high, especially compared to the other error statistics. The explanation is similar as for P_{wave}, it is due to the influence of the peaks in the power production during fast changing wave conditions and more extreme events (Table I and Fig. 7).

Above all, figures show that predictions of Pelamis, Wave Dragon and Wavestar power productions are acceptable.

2) *Combined P_{prod}*: the last row of Table VII reveals the best forecast occurs when considering the combined production of the three devices. The *NBias*, *NRMSE* and $SI_{unbiased}$ improve compared to those of each single device.

Moreover, not only the quality indices show a more accurate forecast but also a high combined mean production.

Above all, the combined production provides the best compromise between forecast accuracy, as for Pelamis and Wave Dragon, and high mean production, as for Wavestar.

A good overview of forecast accuracy of the WECs' P_{prod} can be found in Fig. 8 to Fig. 10.

To compare these, Fig. 11 shows the evolution of the 12 hours forecast H_{m0}, T_{02} and P_{wave} and buoy-measured H_{m0}, T_{02} and P_{wave} over the same 3-day period. The three wave parameters oscillate around their mean values, providing a real representation of the typical sea states at Hanstholm during a winter month.

Fig. 8 and Fig. 9 illustrate the differences between forecast P_{prod} and theoretical P_{prod} of Pelamis, Wave Dragon and Wavestar, for a *T-hour* of 12 hours and 36 hours, respectively. The comparison of both figures shows that the best forecast occurs for a *T-hour* of 12 hours. Here there are some periods where the predictions coincide with the theoretical production. Then, although the errors for the 36-hour forecast are higher, they do not exceed 30% of inaccuracy.

Wave Dragon shows the lowest errors among the three devices and Wavestar the largest. This can be explained due to the more limited working conditions of Wavestar compared to Pelamis and Wave Dragon (Table II).

Fig. 10 depicts the 12, 24 and 36 hours P_{prod} forecast and the theoretical P_{prod} for the combination of the three devices. For most samples the 12 hour forecast is the most accurate.

Then, comparing Fig. 8 to the 12-hour forecast combined P_{prod} (Fig. 10, dashed dark blue line) and similarly, Fig. 9 to the 36-hour forecast combined P_{prod} (Fig. 10, dashed green line), it can be concluded that Fig. 10 generally provides smaller errors than Fig. 8 and Fig. 9. In other words, the combined power production results in an overall better forecast accuracy.

The global improvement of the error statistics by the combined power output confirms that the response of each WEC to the wave climate is different.

Moreover, a relevant finding is that the errors in the forecast of wave parameters H_{m0} and T_{02} do not accumulate but instead cancel-out when calculating the power production of each device. This is a major advantage to take into account in the short future, where the different solutions proposed for wave energy extraction should be considered attractive for the electricity market.

To finalize the discussion, there are three important limitations to this study. First, the selected WECs have been designed for more energetic wave climates than at Hanstholm Therefore, the performances of the devices at this location are different than from those expected at more powerful sites, and thus, their predictability might be compromised. Moreover, comparisons among the performances of the devices should be avoided and cannot be conclusively drawn from these results, as the power productions shown are merely theoretical.

The second limitation is that the use of three WECs reflects the power production by those devices, which embraces different working principles, but not all existing wave conversion technologies.

The third limitation is that this study is not a resource assessment of Hanstholm site nor of the North Sea. Note the analysed data comprise of a 3-month period.

V. Conclusions

Examining the accuracy of wave energy forecasts plays a major role in the integration of wave energy into the electric grid. Waves predictability is related to the electricity market. Current rules of the Danish day-ahead market require the prediction of the following 12 to 36 hours electricity generation.

According to this, the paper has analysed the correlation of:

i) Forecast and buoy-measured wave parameters;
ii) Forecast based and buoy-measured based normalised power productions of three WECs;
iii) Forecast based and buoy-measured based normalised power productions of a combination of the three WECs.

The simultaneous and co-located forecast and measured wave parameters at Hanstholm site, Denmark, during a non-continuous autumn and winter 3-month period, along with the power matrices of the devices, have formed the basis of the study.

The selected WECs have been Pelamis, an offshore floating heaving and pitching articulated device, Wave Dragon, an offshore floating overtopping technology, and Wavestar, a near-shore multi-point absorber. They have been chosen due to their differences in their working principles.

Results indicate accuracies (in terms of unbiased scatter index) in the 12 to 36 hours forecast horizon of:

i) 22%, 11% and 74% for the wave parameters H_{m0}, T_{02} and P_{wave}, respectively;
ii) 37%, 39% and 54% for the normalised theoretical power productions of Pelamis, Wave Dragon and Wavestar, respectively; with normalised mean power productions of 0.33, 0.33 and 0.44.
iii) 36% for the combined normalised theoretical power production of the three devices, with a normalised mean power production of 0.37.

The novelties of this study have been first, examining wave parameters predictability; second, comparing forecast based and buoy-measured based power productions; third, considering the individual as well as the combined power output of three different WECs, and fourth, locating the study in the North Sea waters, an area with increasing interest on wave energy.

Two main conclusions can be drawn from the results: firstly, wave parameters such as H_{m0} and T_{02} can be predicted accurately in the given energetic sea conditions, and secondly, the combined power production from different wave energy technologies provides the best compromise between forecast accuracy and high mean power production.

The latter finding is particularly important at this stage of development of the wave energy sector: it reveals there will probably be more than one established technology for wave energy utilization, it suggests to diversify R&D grants among the different technologies, it indicates the strategy to follow within energy planning processes and it provides a good overview on the parameters to be improved to increase predictability of WECs' production.

These conclusions of the paper suggest two further studies. First, the examination of the predictability of combinations of co-located WECs and wind energy turbines. This will address the delay between wave and wind energy and the comparison of the predictability of both sources. The second study will examine the error statistics of the short-term (0-6 hours) forecast, in comparison to the analyzed day-ahead forecast. This topic is also of great importance to TSOs' electric grid operation.

Furthermore, the on-going prototype tests at Hanstholm can be used to complement the studies by providing actual power production data.

Last but not least, further improvement is expected on the knowledge of device developers about the power production of their devices. This will ultimately decrease the uncertainty on the power matrixes and thus, on the predictability of the actual power to be produced by the devices.

Nevertheless, current rules of the electricity market may have to change to accommodate larger amounts of renewable sources without increasing balancing costs.

ACKNOWLEDGMENT

The first author gratefully acknowledges the financial support from the European Commission through the 7th Framework Programme (the Marie Curie Initial Training Network WaveTrain2 project, grant agreement number 215414) which made this work possible.

The authors are also very grateful to Pelamis, Wave Dragon and Wavestar, whose inputs to the study have been crucial. Measurements at Hanstholm have been made available courtesy of Kystdirektoratet, Denmark.

REFERENCES

[1] Nord Pool Spot, *"The Nordic Electricity Exchange and the Nordic Model for a Liberalised Electricity Market,"* Nord Pool Spot, Denmark, 2009.

[2] EREC, "*Mapping Renewable Energy Pathways towards 2020,"* European Renewable Energy Council (EREC), 2011.

[3] IEA, "*Innovative Electricity Markets to Incorporate Variable Production,"* IEA – Renewable Energy Technology Deployment, 2008.

[4] (2011) Pelamis website [Online]. Available: http://www.pelamiswave.com/.

[5] (2011) Wave Dragon website [Online]. Available: http://www.wavedragon.net.

[6] (2011) Wavestar website [Online]. Available: http://www.wavestarenergy.com/.

[7] H.C. Soerensen and J. Fernandez Chozas, *"The Potential for Wave Energy in the North Sea,"* International Conference on Ocean Energy (ICOE), Spain, 2010.

[8] Ramboll**,** *"Kortlægning af Bølgeenergiforhold i den Danske del af Nordsøen,"* Ramboll, Dansk Hydraulisk Institut, Danamrsk Meteorologiske Institut, 1999.

[9] Ramboll, *"Bølgekraft - forslag til forsoeg og rapportering,"* Ramboll, 1999.

[10] K. Nielsen and T. Pontes, "*Generic and Site-related Wave Energy Data,"* Final technical report, OES-IEA Document No: T02-1.1., 2010.

[11] L. Margheritini, *"Review on available information on waves in the DanWEC area, (DanWEC Vækstforum 2011)," DCE Technical Report No. 135, Aalborg University, 2012.*

[12] (2011) Danish Wave Energy Centre website. [Online]. Available: http://www.danwec.com/.

[13] (2011) DEXA website. [Online]. Available: http://www.dexa.dk/

[14] J. Kirkegaard et al., *"Metocean forecasting for ports and terminals,"* Port Infraestructure Seminar, The Netherlands, 2010.

[15] ECI, *"Variability of UK Marine Resources,"* Environmental Change Institute, University of Oxford, The Carbon Trust, 2005.

[16] F. Fusco, G. Nolan and J.V. Ringwood, *"Variability reduction through optimal combination of wind/wave resources - An Irish case study,"* Energy 35, pp. 314-325, 2010.

[17] L.H. Holthuijsen, "*Waves in Oceanic and Coastal Waters,"* Cambridge, 2007.

[18] H. C. Soerensen et al., "*Bølgekraftanlæg ved Horns Rev – Screening (Wave energy deployment at Horns Rev Wind Farm,"* (partly in Danish), Copenhagen, 2005.

[19] M. Rugbjerg, O.R. Sørensen and V. Jacobsen, *"Wave forecasting for offshore wind farms,"* 9th International Workshop on Wave Hindcasting and Forecasting, Canada, 2006.

[20] E.D. Stoutenburg, N. Jenkins, M.Z. Jacobson, *"Power Output Variability of Co-located offshore wind turbines and wave energy converters in California,"* Renewable Energy, 2010.

[21] R. Gross, et al., *"Renewables and the grid: understanding intermittency,"* Energy 160, pp. 31-41. Proceedings of the Institution of Civil Engineers, 2007.